Running title: VEGF-A_{165}b prevents diabetic neuropathic pain

Vascular endothelial growth factor-A_{165}b prevents diabetic neuropathic pain and sensory neuronal degeneration.

[a,b]R.P. Hulse, [a,c]N. Beazley-Long, [c,d]N. Ved, [b]S.M. Bestall, [a]H. Riaz, [a]P. Singhal, [e]K. Ballmer Hofer, [a]S.J. Harper, [a,b]D.O. Bates and *[a,c]L.F Donaldson.
[a]School of Physiology and Pharmacology, University of Bristol, Bristol BS8 1TD, [b]Cancer Biology, School of Clinical Sciences, University of Nottingham, Nottingham NG7 2UH, [c]Arthritis Research UK Pain Centre and School of Life Sciences, The Medical School QMC, University of Nottingham, Nottingham NG7 2UH. [d]Institute of Ophthalmology, 11-43 Bath St, London EC1V 9EL. [e] Paul Scherrer Institute, Villingen, Switzerland.

*Correspondence author
Arthritis Research UK Pain Centre, School of Life Sciences
The Medical School, QMC
University of Nottingham
Nottingham
NG7 2UH

Tel: +44 (0)115 8230158
Email: Lucy.Donaldson@nottingham.ac.uk

Key words: diabetic neuropathy; rat; VEGF-A_{165}b; streptozotocin; TRPA1.

Abstract

Diabetic peripheral neuropathy affects up to half of diabetic patients. This neuronal damage leads to sensory disturbances, including allodynia and hyperalgesia. Many growth factors have been suggested as useful treatments for prevention of neurodegeneration, including vascular endothelial growth factor family. VEGF-A is generated as two alternative splice variant families. The most widely studied isoform, VEGF-A_{165}a is both pro-angiogenic and neuroprotective, but pro-nociceptive and increases vascular permeability in animal models. Streptozotocin-induced diabetic rats develop both hyperglycaemia and many of the resulting diabetic complications seen in patients, including peripheral neuropathy. Here we show that the anti-angiogenic VEGF-A splice variant, VEGF-A_{165}b, is also a potential therapeutic for diabetic neuropathy. Seven weeks of VEGF-A_{165}b treatment in diabetic rats reversed enhanced pain behaviour in multiple behavioural paradigms and was neuroprotective, reducing hyperglycaemia-induced activated caspase 3 levels in sensory neuronal subsets, epidermal sensory nerve fibre loss and aberrant sciatic nerve morphology. Furthermore, VEGF-A_{165}b inhibited a streptozotocin-induced increase in Evans Blue extravasation in dorsal root ganglia (DRG), saphenous nerve and plantar skin of the hind paw. Increased TRPA1 channel activity is associated with the onset of diabetic neuropathy. VEGF-A_{165}b also prevented hyperglycaemia-enhanced TRPA1 activity in an *in vitro* sensory neuronal cell line indicating a novel direct neuronal mechanism that could underlie the anti-nociceptive effect observed *in vivo*. These results demonstrate that in a model of type I diabetes VEGF-A_{165}b attenuates altered pain behaviour and prevents neuronal stress, possibly through an effect on TRPA1 activity.

Introduction

Diabetes mellitus affects 6.7% of European and 10.5% of the US populations and results in a myriad of debilitating complications that constitute an increasing burden on healthcare systems. A major complication is diabetic neuropathy, affecting up to 50% of diabetic patients [1]. Hyperglycaemia affects sensory afferents, and autonomic and motor nerves [2], influencing unmyelinated [3] and myelinated [4] fibre function, leading to autonomic and motor dysfunction, and altered proprioception and nociception. Nociceptors are rendered more sensitive to activation as a result of changes in the local microenvironment, such as compromised vascular perfusion and/or direct actions upon neurons. Sensory neurons are particularly susceptible to hyperglycaemic damage, due to a lack of insulin-regulated glucose uptake [5], and are also affected by the generation of reactive metabolites such as oxidative or glycosylated by-products under hyperglycaemic conditions [6]. Exposure to persistently high glucose levels in humans and in rodent models leads to classical signs of diabetic neuropathy, axonal atrophy and demyelination, reductions in conduction velocity and epidermal innervation, and symptoms of allodynia, (pain in response to normally non-painful stimuli), hyperalgesia (more severe pain in response to a normally painful stimulus), burning, or on-going pain. Sensory neuronal damage and loss may ultimately lead to hypoalgesia or anaesthesia [7]. A number of mechanisms have been proposed to underlie diabetes-induced neuro-pathology [2, 5], including activation of transient receptor potential ankyrin 1 (TRPA1) channels [8], blockade of which attenuates both diabetes-induced peripheral neuronal loss and neuropathic pain [9].

Neuronal complications are attributed to both microvascular damage and reduction in neural trophic support, for example both nerve growth factor (NGF) [10] and vascular endothelial growth factor-A (VEGF-A) [11] are reduced. VEGF-A_{165}a is the archetypal pro-angiogenic factor that also has neuroprotective capacity in experimental diabetes [12]. The products of the *vegf-a* gene consist of two isoform families; VEGF-A_{xxx}a and VEGF-A_{xxx}b (xxx relates to amino acid number), generated by alternative pre-mRNA splicing that differ only in their terminal six amino acid sequences. While each family's predominant isoform, VEGF-A_{165}a and VEGF-A_{165}b respectively, is neuroprotective for sensory neurons [13, 14], VEGF-A_{165}a is also pro-nociceptive [15]. In contrast, VEGF-A_{165}b is anti-angiogenic and anti-nociceptive yet also neuroprotective, *in vivo* and *in vitro*, through alternative VEGFR2 activation and signalling mechanisms [13, 16-18]. In diabetic neuropathy, intra-epidermal nerve fibre loss and the severity of pain are related to the degree of decrease in VEGF and VEGFR2 expression, suggesting a relationship between VEGF-A and diabetic neuronal damage [19]. Therefore we tested the hypothesis that the anti-angiogenic, neuroprotective, anti-nociceptive VEGF-A isoform, VEGF-A_{165}b, protects against neuronal damage and pain in a model of Type I diabetes. Our results are the first to demonstrate that in this diabetes model, systemic delivery of recombinant human VEGF-A_{165}b can reverse pain-like behaviours and prevent peripheral neuropathy.

Research Design and Methods

Thirty-seven female Sprague Dawley rats (~250g) were used in this study in accordance with the UK Home Office Animals (Scientific Procedures) Act 1986 and amendments (2012), and were approved by the Universities of Bristol and Nottingham AWERBs (Animal Welfare and Ethical Review Boards). Diabetes was induced with intraperitoneal (i.p.) injection of streptozotocin (STZ) (50mg/kg) and one third of an insulin pellet (Linshin, Canada) was implanted in the scruff of the neck using the supplied trocar (Linshin, Canada) under isoflurane anaesthesia (2-3% in O_2) [20]. For the first 24h animals had *ad libitum* access to saturated sucrose solution, animals had *ad libitum* access to standard chow throughout, were regularly weighed, and housing and drinking water regularly checked over the 9 week study. Experimental groups were diabetic animals ± saline (i.p. n=14), or recombinant human VEGF-A_{165}b (20ng/g body weight, i.p. twice weekly from week 1, n=12) [13] and untreated naïve animals (n=11).

Nociceptive Behavioural Testing

Rats were habituated to the behavioural testing environments for 2 weeks (enclosures with metal mesh or Perspex floors) and for 10 minutes before the start of each session. The operator was blind to treatment throughout.

Mechanical withdrawal thresholds: von Frey (vF) monofilaments of increasing forces were applied to the plantar surface of the hind paws. Each monofilament was applied 5 times to generate a force:response (withdrawal) relationship and the 50% withdrawal threshold was calculated. Cold nociception: a single drop of acetone was applied to the plantar surface of the hind paw 5 times with quantification of licking/shaking nociceptive behaviours [21] (positive response = 1, no response = 0, maximum = 5). Heat nociception: withdrawal to heat was determined using the Hargreaves test [22]. The intensity of the radiant heat source was set and remained constant for the duration of the study. Each hind paw was stimulated three times and mean withdrawal latency was calculated. Mechanical and thermal nociceptive behaviours were tested weekly throughout the study. Response to a noxious chemical stimulus was determined by subcutaneous injection (dorsal surface of hind paw) of 0.5% formalin prior to diabetes induction [20], and at 2 and 7 weeks after diabetes onset. This is a low concentration of formalin, that induces only a slight and brief acute phase (0-15 min), and no second phase (15-60 min) response in normal rats (Fig. 2D), and does not induce prolonged sensitization.

Immunofluorescence and Toluidine Blue Histology

After 7 weeks, animals were terminally anaesthetized (sodium pentobarbital 60mg/kg i.p.) and transcardially perfused, with either phosphate buffered saline (PBS) followed by 4% paraformaldehyde in PBS (PFA; pH7.4) for immunofluorescence or PBS followed by 2.5% glutaraldehyde in cacodylate buffered saline (CBS, pH7.4) for sciatic nerve myelinated fibre counts. L4&5 DRG and hind paw plantar skin were removed, post-fixed overnight (4% PFA at 4^{o}C), and transferred to 30% sucrose overnight at 4^{o}C. Tissue was embedded, frozen and stored at -80^{o}C until sectioning and processing. Cryosections were cut at 8µm (DRG) or 20µm (plantar skin), mounted on slides (Superfrost plus, VWR international), washed (PBS), and incubated in blocking solution (5% bovine serum albumin, 10% foetal calf serum, 2h at room temperature) followed by primary antibodies (see below) in blocking solution, overnight at 4^{o}C. Sections were washed with PBS, incubated in secondary antibodies in PBS + 0.2% Triton X-100 at room temperature for 2h, coverslipped in Vectorshield mounting media (Vector Laboratories; +DAPI). Sciatic nerve was removed, post-fixed in 2.5% glutaraldehyde and CBS (pH7.4) at 4^{o}C until processed by washing in CBS, incubation in 1% osmium tetroxide in 0.1M CBS, and CBS wash. Samples were dehydrated, embedded in resin, and semi-thick sections (1µm) stained with toluidine blue [23].

Primary antibodies and dilutions were: polyclonal rabbit, anti-activated caspase III (AC3; 1 in 500, NEB); monoclonal mouse, anti-NeuN (1 in 200, Millipore); isolectin B_4-biotin conjugated (IB4; 1 in 500, Sigma-Aldrich); monoclonal mouse, anti-neurofilament 200 (NF200; 1 in 1000, Sigma-Aldrich); polyclonal rabbit anti-PGP9.5 (1 in 200, Ultraclone); polyclonal rabbit anti-NSE-1 (neuron-specific enolase-1, 1 in 1000, VWR); monoclonal rabbit anti-VEGF receptor 2 (Cell Signaling 55B11 1 in 200); goat polyclonal anti-actin (Santa Cruz SC-1616 2µg/ml). Secondary antibodies for immunofluorescence were Alexa Fluor 488-conjugated chicken anti-mouse, Alexa Fluor 555-conjugated donkey anti-rabbit and streptavidin-conjugated Alexa Fluor-488 (all Invitrogen, UK). Controls included replacement of primary antibody with species and concentration-matched IgG or pre-incubation with appropriate blocking peptide (activated/cleaved caspase III, NEB). Secondary antibodies for Western blotting were Licor IRDye 680RD donkey anti-rabbit, 1 in 5000 and donkey anti-goat Licor IRDye 800CW, 1 in 5000.

For DRG (n=3) and plantar skin (n=3) analyses, a minimum of 5 randomly selected non-serial images from at least 5 sections from each animal in each treatment group, at a magnification of x20 (plantar skin) or x10 (DRG). In skin all PGP9.5 positive nerve fibres were counted per image area (35mm^2). In DRG the mean number of neurons (identified by NeuN/Neurofilament) counted per animal was ~800. Myelinated axon counts were performed on a minimum of 5 random non-serial images per section, 5 sections per animal (a mean of ~450 axons per animal).

Evans Blue Extravasation

In vivo vascular dysfunction was evaluated using Evans' Blue dye perfusion [24]. Seven week diabetic + saline, diabetic + VEGF-A_{165}b and age-matched controls (n=5 each) were terminally anesthetized (ketamine/medetomidine i.v. 50 mg/kg) and infused with Evans Blue dye i.v. (Sigma-Aldrich, 45 mg/kg) Two minutes post-infusion, 0.2mL arterial blood was withdrawn, followed by subsequent 0.1mL withdrawals every 15 minutes for 2 hours. After 2 hours of Evans' Blue dye circulation, 0.2mL blood was withdrawn from the heart followed by cardiac perfusion of 50mL saline at 120mmHg. DRG L3, 4 & 5, left saphenous nerve and left plantar skin were excised and weighed to determine their wet weight. Tissue was then dried at 70˚C overnight and weighed to determine dry weight. To determine Evans' Blue extravasation, dried tissue was incubated in 0.15mL formamide (Sigma Aldrich) at 70˚C overnight. Blood samples were centrifuged at 12,000 rpm for 45 minutes at 4˚C, and the supernatant from tissue and blood samples were analysed at 620nm. Evans' Blue extravasation (estimated as permeability-surface area product, PA) was calculated as Evans' Blue wet weight solute flux (µg/h/g) divided by time-averaged plasma Evans Blue concentration (µg/mL) multiplied by total time (h).

Primary Dorsal Root Ganglia Sensory Neuronal Cultures

Adult rat Wistar rats were perfused transcardially with PBS under anaesthesia (sodium pentobarbital 60mg/kg, i.p.) and T1-L6 DRG were extracted, enzymatically and mechanically dissociated, and cultured on poly-l-lysine/laminin coated glass coverslips in Ham's F12 plus 1x N2 supplement (Life Technologies), 0.3% BSA + 1% pen/strep. After cell attachment, mitotic cells were inhibited with 30µg/mL 5-fluoro-2'-deoxyuridine. Cultures were pre-treated overnight (18hrs) with 2.5nM VEGF-A_{165}b or vehicle as previously described [13], then incubated under either high glucose (final concentration 50mM) or a basal neuronal culture glucose level (10mM) [25] for 6h. Proportions of activated caspase III (AC3)-positive DRG neurons (co-labelled NSE-1) were determined by immunofluorescence as previously described.

Epifluorescence imaging was performed on a Nikon Eclipse E400 microscope equipped with x40 objective lens and a Nikon DN100 camera. Confocal imaging was performed on Leica TCS SPE confocal microscope. Images were acquired using x63 oil immersion objective lens and Leica application suite. All imaging was performed at room temperature. Computer-aided analysis of images was performed using ImageJ (NIH, Bethesda, MD; available at http://rsb.info.nih.gov/nih-image). In each instance the analyser was blinded to treatment group.

Immortalised Neuronal Cell Line (50B11) Cell Culture

TRPA1 channel activation was assayed in immortalized embryonic rat sensory neurons, 50B11, in line with the requirements of UK legislation and the 3Rs. 50B11 cells were maintained under previously published conditions [26]: Neurobasal media (Invitrogen), supplemented with foetal bovine serum (10%), glutamine (0.55mM), B27 supplement and additional glucose (11mM) making the total glucose concentration 36mM (basal glucose). Incubation with lower, more physiological glucose concentrations *in vitro* affects their neuronal phenotype, impairing normal neurite outgrowth (Bestall et al, unpublished data). For these cells therefore, this high glucose level (compared with *in vivo*) is a requirement for normal function, and therefore considered "basal". 50B11 cells were plated into 96 well plates and incubated for 2 days, then differentiated with 75µM forskolin maintained in the medium for at least 24h, after which cells were incubated overnight with the following reagents: 2.5nM VEGF-A_{165}b, PBS vehicle, 200nM PTK787 (VEGFR2 inhibitor, in 0.02% DMSO), 0.02% DMSO control, 8.05µg/mL DC101 (rat monoclonal anti-mouse VEGFR2, BioXcell) or 8.05µg/mL rat IgG control. *In vitro* high glucose conditions were maintained for 24h, with addition of a further 30mM glucose (final concentration 66mM) to the media, or 30mM mannitol to control for osmotic effects. After differentiation and incubation under experimental conditions, cells were loaded with Fluo-4 (Invitrogen) in Hank's balanced salt solution containing 20mM HEPES and 2mM $CaCl_2$ for 1h. The TRPA1 agonist allyl isothiocyanate (AITC in PBS, Sigma-Aldrich) was used to activate TRPA1 channels and calcium fluorescence measured in a Wallac 1420 Victor 3 multi-plate reader (Perkin Elmer) at 37^{o}C. A TRPA1 antagonist, AP-18 (Tocris, UK) was used to determine the specificity of AITC in this assay. Baseline readings were determined prior to stimulation by 100µM AITC, and after AITC application, sequential fluorescence emission values were recorded. The time of the first reading was ~25s after AITC application.

The effect of high glucose treatment or 300µM AITC for 24h (application twice at 12h intervals) on AC3 in 50B11 cells was also determined. After 24h differentiation with forskolin, 50B11 cells were treated for 24h, then fixed and stained for AC3 as previously detailed. Total image AC3 fluorescence intensity was expressed over total DAPI fluorescence (total cell nuclei) intensity to account for differences in cell number.

Western Blotting

The presence of VEGF receptor 2 (VEGFR2) in 50B11 cells was confirmed with Western blotting. 50B11s grown in either normal (36mM) or high (66mM) glucose were lysed and protein extracted in the presence of phenylmethylsulfonyl fluoride and proteinase inhibitors. Protein lysate as electrophoresed on 10% SDS-PAGE gels, blotted on PVDF membrane by wet transfer and incubated for 24 hours at 4^{o}C with anti-VEGFR2 antibody in blocking buffer (Tris buffered saline, 0.1% Tween-20, 5% bovine serum albumin). After secondary antibody incubation for 1 hr at room temperature in blocking buffer, blots were imaged using a Licor imaging system. Protein loading differences between wells were controlled for by probing of the same blot for actin. Protein lysate from endothelial cells was used as a positive control for VEGFR2 expression.

Analysis and Statistical Analysis

Acquired data were processed and graphed using Microsoft Excel 2007 and GraphPad Prism v5-6. Data are shown as mean±SEM unless otherwise stated. Three or more groups were compared using between subjects one or two way ANOVA with post-hoc Bonferroni tests, and two groups were compared using Wilcoxon signed rank tests, as stated in the Figure legends. Representative data values for outcome measures are given in Table 1.

Results

Recombinant human VEGF-A_{165}b prevented diabetic neuropathic pain *in vivo*

As previously reported [20], STZ-injection with low dose insulin supplementation resulted in a maintained hyperglycaemia (Fig 1A) and body weight (Fig 1B) over the duration of the study. Also as previously reported [20], STZ treatment with low-dose insulin supplementation resulted in a rapid (1-2 weeks) and significant lowering of mechanical-stimulus withdrawal thresholds (mechanical allodynia), maintained for the duration of the study (Fig. 1C). In addition, diabetic animals developed significant cold allodynia (Fig. 1D), and heat hyperalgesia (Fig. 1E). Biweekly, systemic VEGF-A_{165}b treatment significantly reversed the initial changes in mechanical allodynia (Fig. 1C), prevented the onset of cold allodynia (Fig. 1D) and reversed the heat hyperalgesia (Fig. 1E). Chemical nociception in response to a low dose of formalin (0.5%) was enhanced in diabetic animals, measured at week 2 (Fig. 1F). This enhanced acute chemo-nociception at week 2 was ameliorated by VEGF-A_{165}b treatment (Fig. 1F). The significant increase in chemo-nociceptive behaviour in diabetic rats was lost by week 7 (Fig. 1F). No significant second phase behaviour (indicative of central sensitization) was observed in response to formalin in any animals at any time point.

Recombinant human VEGF-A_{165}b protected sensory neurons against hyperglycaemic damage *in vivo* and high glucose treatment *in vitro*

Incubation of adult rat primary DRG neurons in increased glucose conditions for 6h resulted in an increase of the percentage of neurons expressing activated caspase 3 (AC3) (Fig. 2A & B; basal glucose = 26.3±3.5%, high glucose = 53.0±6.1%), indicating neuronal stress under these conditions, which was blocked by recombinant human VEGF-A_{165}b (Fig. 2B; high glucose ± VEGF-A_{165}b = 35.0±2.3%). VEGF-A_{165}b alone had no effect on expression of AC3. We then determined whether VEGF-A_{165}b could protect sensory neurons against damage *in vivo* in the rodent model of Type I diabetic neuropathy in which VEGF-A_{165}b had inhibited pain responses (Fig. 1). Figure 2C & D shows that the number of AC3-expressing L5 (Fig. 2C-F) and L4 (not shown) DRG neurons was increased in diabetic rats *in vivo* compared to naïve and this was reduced by VEGF-A_{165}b treatment, predominantly in the small diameter population (Fig. 2E). Furthermore, there was an increase in the total number of smaller DRG neurons (<400μm^2 PGP9.5-positive DRG neurons) within the diabetic animals versus age-matched controls (Fig. 2F). VEGF-A_{165}b treatment prevented this increase in number of smaller DRG neurons. Co-staining demonstrated that there was increased AC3 staining in nociceptive small IB_4-reactive neurons (Fig. 3A & B) and also in myelinated neurons (neurofilament (NF200)-positive Fig. 3C & D). VEGF-A_{165}b treatment reversed the increased AC3 expression in both neuronal groups (Fig. 3B & D). A reduction in epidermal innervation is a diagnostic hallmark of diabetic neuropathy [27]. Seven weeks after STZ injection, there were fewer PGP9.5-positive nerve terminals at the dermal/epidermal border and entering the epidermis in hind paw plantar skin (Fig. 4A, arrows), which was reversed with VEGF-A_{165}b treatment at week 7 (Fig. 4B). Langerhans cells, inflammatory cells reported to increase in number in diabetic patients [28], were also increased in the epidermis of diabetic rats at week 7 (Fig. 4A, arrowheads) and this was also significantly reduced by VEGF-A_{165}b treatment (Fig. 4C).

Morphological changes, including axon diameter and myelin structure of sciatic nerve, have been reported in $SOD1^{-/-}$ and db/db mice [23], and are thought to result from hyperglycaemic damage of the neuronal myelin through either structural or compositional alterations [23]. In diabetic rats, we found similar changes (Fig. 5A), in that there was an overall reduction in myelinated axon cross-sectional area in the sciatic nerve (Fig. 5B) compared to naïve animals, and this was reversed by VEGF-A_{165}b. The reduction in the number of 'medium sized' fibres with cross-sectional areas <90µm^2 but >30µm^2 (and an increase in the number of small myelinated fibres with areas <30µm^2 (Fig. 5C), may reflect a reduction in larger axon size resulting in an apparent increase in the number of smaller myelinated fibres. Again, as previously observed [23], there was an increase in the number of axons with gross indications of aberrant myelin morphology in diabetic animals (Fig. 5D &E; asterisks in 5A), which was reversed by VEGF-A_{165}b (Fig. 5E). Furthermore, NF200-positive neuronal cell bodies in L5 DRG had significantly smaller cross-sectional areas in the diabetic group compared to the naïve age-matched control group (Fig. 5F & G). VEGF-A_{165}b treated prevented this reduction in size of the neurofilament sensory neuronal population.

VEGF-A_{165}b prevented STZ-induced increase in Evans Blue extravasation in DRG, the saphenous nerve and hind paw plantar skin.

Diabetic animals had a significant increase in Evans Blue extravasation in DRG (Fig. 6A), and saphenous nerve (Fig. 6B), with a trend to suggest an increase in theplantar hind paw skin (Fig. 6C) compared to naïve animals. Biweekly treatment of VEGF-A_{165}b significantly reduced Evans Blue extravasation in these tissues compared to vehicle-treated animals (Fig. 6A-C). Data are displayed as permeability–surface area coefficient (PA) values.

TRPA1-mediated calcium fluorescence was affected by VEGF-A_{165}b *in vitro*.

Diabetic neuronal terminal loss and pain are suggested to occur, at least in part, through sustained activation of C-fibre nociceptors [3] particularly those expressing the non-selective cation channel, TRPA1 [9]. Immortalized rat sensory neurons (50B11 [26]) express nociceptive channels such as functional TRPV1, P2X [26], TRPA1 (Fig. 7A), and also receptors for VEGF (Fig. 7B). VEGF receptor-2 expression was not changed under high glucose conditions (not shown). The TRPA1 agonist AITC evoked a concentration-dependent increase in intracellular calcium levels in 50B11 cells maintained under basal glucose concentrations [26] (Fig. 7A). AITC has been shown to activate TRPV1 as well as TRPA1 [29]. The TRPA1 antagonist, AP-18 significantly blocked the calcium response to 100µM AITC (Fig. 7B & C) indicating that in this assay AITC stimulated exclusively TRPA1 to increase intra-cellular calcium. The response to 100µM AITC was significantly inhibited by pre-treatment with VEGF-A_{165}b for 24h (Fig. 7D & E). AITC treatment (300µM, 24h) also caused a significant increase in AC3 fluorescence intensity measured in 50B11 cells (Fig. 7F & G).

Exposure of 50B11 cells to high glucose treatment caused a significant increase in AC3 fluorescence intensity (Fig. 8A & B). High glucose also enhanced the level of intracellular calcium in response to 100µM AITC stimulation indicating either altered channel kinetics or altered calcium extrusion under high glucose treatment, an effect that was not attributable to an osmotic effect of the additional glucose (Fig. 8C & D). Treatment with VEGF-A_{165}b significantly inhibited AITC-evoked calcium fluorescence under high glucose conditions (Fig. 8E & F). Under high glucose conditions, the effect of VEGF-A_{165}b on the calcium response was blocked by a VEGFR2 tyrosine kinase inhibitor (PTK787, 200nM; Fig. 8G), and a VEGFR2 receptor-neutralizing antibody (DC101; Fig. 8H).

Discussion

Diabetic patients complain of abnormal sensations, including allodynia and hyperalgesia. Diabetic neuropathy is also associated with loss of sensation as peripheral sensory nerve terminals are lost from the dermis and epidermis. Classically these symptoms occur in the extremities e.g. toes, affecting more proximal regions as the disease progresses. Thus diabetic neuropathy is classically characterized by peripheral nerve fibre degeneration in both myelinated and unmyelinated sensory nerves with abnormal pain perception. A number of transgenic and inducible rodent models of diabetes show similar sensory abnormalities [30]. STZ-induced hyperglycaemia leads to a pronounced neuropathic pain phenotype in the rat [20], and high levels of blood glucose lead to the development of mechanical and cold allodynia, and heat hyperalgesia. Heightened pain responses may arise as a result of damage to the peripheral nervous system from direct actions of glucose [5], metabolite production [9], inflammation [31], or microvascular damage and other associated micro-environmental changes [32]. In our study, STZ-treated rats developed hyperglycaemia, mechanical and cold allodynia, heat hyperalgesia and altered plasma extravasation around peripheral neurons. Furthermore DRG sensory neurons exposed to high levels of glucose both *in vitro* and *in vivo* had increased expression of the stress marker, activated caspase-3 (AC3), in agreement with other studies showing neuronal stress to DRG neurons in response to hyperglycaemia [25]. We also observed a change in the size profile of DRG neurons with diabetic animals having a greater percentage of smaller diameter neuronal cell bodies than naïve animals. STZ treatment also led to a reduced number of nerve terminals at the dermal-epidermal junction in hind paw plantar skin indicating a loss of innervation, a distinct feature of diabetic neuropathy that affects both large and small fibre neurons [19]. The sciatic nerve contains sensory fibres and motor and autonomic axons; both sensory and autonomic terminals could be lost from skin, and these cannot be distinguished purely on the fibre profiles studied here. In our study the observed increase in small myelinated fibre profiles in sciatic nerve trunk may represent some demyelination of larger fibres [23], and hence smaller apparent cross sectional area both in the nerve fibre and somata. Myelin damage could affect sensory fibres or motor axons, although hyperglycaemia has been shown to affect sensory fibres to a greater extent than motor axons [33]. The impact of the diabetic state on myelinated sensory fibres is indicated by the observed AC3 expression in neurofilament (NF200)-containing DRG neurons and by the decrease in the size of NF200+ve neuronal cell bodies. Small fibre neuropathy in diabetes is also associated with an increased epidermal recruitment of Langerhans cells [28], which is consistent with evidence of cell stress (AC3 expression) in the smaller diameter neurons. Langerhans cells are dendritic cells that increase their expression of PGP9.5 following denervation and inflammation [34]. Changes in Langerhans cell number could be attributable to peripheral denervation, and/or altered capillary permeability and plasma/albumin extravasation resulting from local inflammatory responses.

Both endoneurial capillary permeability and oedema can be seen in models of STZ-induced diabetes [35]. After 7 weeks of hyperglycaemia, Evans' Blue extravasation significantly increased in sciatic nerve, and DRG, suggestive of an increase in neural perfusion and/or capillary permeability that could be attributable to hyperglycaemic microvascular damage. Although sensory neurons are particularly susceptible to hyperglycaemic injury [36] as they lack insulin-regulated glucose uptake [5], local hypoxia as a consequence of ischaemia resulting from damage to the vasa nervosa may also contribute to peripheral neuropathy [37].

Diabetic rodents have alterations in peripheral growth factors e.g. NGF [10] and VEGF [11]. Increased expression of pro-angiogenic VEGF isoforms (increased VEGF-A_{xxx}a vs VEGF-A_{xxx}b) is associated with a number of diabetic complications e.g. retinopathy [38] and nephropathy [39]. In contrast, expression of the VEGF-A family is reduced in sensory neurons in models of STZ-induced diabetic rodents [11]. Furthermore, reduced VEGF-A and VEGFR2 expression correlates with the increased severity of neuropathy in diabetic patients both in terms of pain score and the degree of epidermal innervation [19]. As such a number of studies

have investigated avenues to provide induction of VEGF (VEGF-A and VEGF-C) family expression. In ischaemic and diabetic neuropathy plasmid introduction (AND ROPPER schratsberger REFs) or methods of transcriptional activation PAWSON have led to increased expression of VEGF-A, resulting in rescue of vascular perfusion, which is accompanied by recovery of neuronal function and therapeutic analgesic relieve. However, this approach could result in adverse events e.g. pain as previously reported with splicing dependent events VEGF-A_{xxx}a (hulse et al). Consideration and management of the specific splice isoform ratio are therefore critical.

VEGF-A_{xxx}b is a potent neuroprotective factor for neurons including DRG [13], as is the alternatively spliced variant VEGF-A_{xxx}a, in chemotherapeutic, diabetic and traumatic neuropathies [12, 14]. VEGF-A_{xxx}a and VEGF-A_{xxx}b signal through different downstream pathways on VEGFR2 activation, although both isoform families can act through ERK1/2 to exert neuroprotective actions [13]. A reduction in expression of either VEGF-A isoform family will therefore affect the potential for neuroprotection and/or regeneration. Systemic treatment with VEGF-A_{165}b protein *in vivo* was able to prevent both neuropathic pain and the neuronal changes seen in diabetes that lead to neuropathy including a change in DRG neuronal size profile, loss of nerve terminals, inflammatory cell infiltration into skin, axonal atrophy, and increased Evans Blue extravasation in diabetic animals, possibly by restoring some of the lost trophic support.

TRPA1 is a non-specific cation channel that has been implicated in the neuronal loss seen in diabetic [9], and chemotherapy-induced neuropathy [40]. Blockade of TRPA1 activity attenuates both diabetic neuropathic pain and the associated neuronal terminal loss [9]. TRPA1 is activated by the low formalin concentrations used in this study [41], responses that are sensitized at week 2, and attenuated by VEGF-A_{165}b treatment. Importantly, TRPA1 has been localized to the IB_4 nociceptor subset, neurons that are readily sensitized, are responsible for 'hyperalgesic priming' [42], and as we show, are affected by diabetic neuropathy. Furthermore, TRPA1 sensitization/activation in sensory nerve terminals can result in neurogenic inflammation and increased cutaneous plasma extravasation [43], thus suppression of sensory neuronal sensitization through TRPA1 by VEGF-A_{165}b, acting through VEGFR2 [16], may also underlie the observed effect on plasma extravasation in the skin. VEGF-A_{165}b can antagonize the vasodilatatory effects of VEGF-A_{xxx}a [44] so the observed effect of VEGF-A_{165}b on Evans' Blue extravasation may also be due, at least in part, to direct actions on the vascular tone.

To explore whether VEGF-A_{165}b could exert some of its actions through TRPA1 we used an *in vitro* assay of TRPA1 sensitization. Sensory neurons compromised by a peripheral nerve injury (indicated by expression neuronal stress/death/degeneration markers (e.g. AC3)), undergo changes in excitability that underpin neuropathic pain [45]. TRP channels including TRPA1 contribute to peripheral C-fibre nociceptor sensitization in a range of neuropathic [40] and inflammatory conditions [46]. Although the exact function of TRPA1 is still debated, it can be considered as a "universal sensitizer" channel in peripheral nociceptors, contributing to mechanical [46], cold [47] and chemical pain, especially that generated by endogenous metabolites generated in hyperglycaemic conditions [9, 48].

STZ-induced hyperglycaemia causes an increase in endoneurial levels of the toxic glucose metabolite methylglyoxal and methylglyoxal-glycated proteins (advanced glycated end products) [6]. AITC induced an intracellular calcium fluorescence signal in 50B11 immortalised neurons that was further sustained by high glucose treatment. The effect of AITC was blocked by a TRPA1 inhibitor, indicating that calcium entry was mediated by TRPA1 alone. Methylglyoxal is known to induce sustained TRPA1 activity under hyperglycaemic conditions [9, 48], and its production may produce observed sustained TRPA1 activation following high glucose treatment. TRPA1-mediated calcium responses, under normal or high glucose conditions were significantly inhibited by VEGF-A_{165}b, acting through VEGFR2. VEGF-A_{165}b-induced blockade of TRPA1-mediated calcium entry/handling in these high glucose conditions

in vitro could therefore reduce both neuronal damage and the mechanical and thermal pain resulting from TRPA1 sensitization of peripheral nerve terminals.

This study demonstrates that exogenous recombinant VEGF-A_{165}b protein delivered systemically can reverse signs of diabetic neuropathy in the rat. VEGF-A_{165}b was protective against hyperglycaemia-mediated events in diabetic neuropathy, exerting neuroprotective and anti-nociceptive actions on peripheral sensory neurons, possibly through a TRPA1-mediated mechanism. It is therefore important to determine whether control of VEGF-A_{165}b levels, either through exogenous protein therapy, or control of alternative RNA splicing mechanisms [49] represents a novel therapeutic strategy for the treatment of multiple diabetic complications, including diabetic neuropathy.

Clinical perspective

Diabetic complications such as neuropathy affect up to 50% of all diabetics. The pain associated with diabetic neuropathy is a large unmet clinical need due the increasing numbers of diabetics worldwide. Vascular endothelial growth factor-A (VEGF-A) has been suggested to be a possible therapeutic for diabetic neuropathy; this is a family of proteins generated through alternative pre-mRNA splicing that can exert different physiological effects. We show that human recombinant protein VEGF-A_{165}b can ameliorate both diabetic neuronal injury and neuropathic pain in experimental rodents. Therapeutics that alter the VEGF-A isoform complement in favour of VEGF-A_{165}b may be novel treatments for diabetic neuropathy.

Author contributions

RPH, NBL, NV, SMB, HR, PS, KBH performed research, RPH, NBL, NV, SJH, DOB & LFD designed the research and analysed data. RPH, NBL, DOB and LFD wrote the manuscript with contributions from SJH and final approval from all authors.

Acknowledgements and declarations of interest

We thank Ahmet Hoke, John's Hopkins University, and Damon Lowes, University of Aberdeen for the gift of the 50B11 cell line.
LFD, DOB, SJH are co-inventors on patents protecting VEGF-A_{165}b and alternative RNA splicing control for therapeutic application in a number of different conditions. LFD, DOB, SJH are founder equity holders in, and DOB and SJH are directors of Exonate Ltd, a company with a focus on development of alternative RNA splicing control for therapeutic application in a number of different conditions, including diabetic complications.

Funding

This work was supported by Diabetes UK (11/0004192, LFD and DOB), the Wellcome Trust (079736, DOB), The Swiss National Science Foundation (31003A, K.B-H.), Oncosuisse (OC201200-08-2007, K.B-H) and The Richard Bright VEGF Research Trust (DOB, UK Reg. Charity 1095785).

References

1. Obrosova, I.G. (2009) Diabetic painful and insensate neuropathy: pathogenesis and potential treatments. Neurotherapeutics. **6**(4), 638-47.
2. Tomlinson, D.R. and N.J. Gardiner. (2008) Diabetic neuropathies: components of etiology. J Peripher Nerv Syst. **13**(2), 112-21.
3. Chen, X. and J.D. Levine. (2003) Altered temporal pattern of mechanically evoked C-fiber activity in a model of diabetic neuropathy in the rat. Neuroscience. **121**(4), 1007-15.
4. Christianson, J.A., J.M. Ryals, M.S. Johnson, R.T. Dobrowsky, and D.E. Wright. (2007) Neurotrophic modulation of myelinated cutaneous innervation and mechanical sensory loss in diabetic mice. Neuroscience. **145**(1), 303-13.
5. Tomlinson, D.R. and N.J. Gardiner. (2008) Glucose neurotoxicity. Nat Rev Neurosci. **9**(1), 36-45.
6. Duran-Jimenez, B., D. Dobler, S. Moffatt, N. Rabbani, C.H. Streuli, P.J. Thornalley, D.R. Tomlinson, and N.J. Gardiner. (2009) Advanced glycation end products in extracellular matrix proteins contribute to the failure of sensory nerve regeneration in diabetes. Diabetes. **58**(12), 2893-903.
7. Calcutt, N.A., C.G. Jolivalt, and P. Fernyhough. (2008) Growth factors as therapeutics for diabetic neuropathy. Curr Drug Targets. **9**(1), 47-59.
8. Wei, H., M.M. Hamalainen, M. Saarnilehto, A. Koivisto, and A. Pertovaara. (2009) Attenuation of mechanical hypersensitivity by an antagonist of the TRPA1 ion channel in diabetic animals. Anesthesiology. **111**(1), 147-54.
9. Koivisto, A., M. Hukkanen, M. Saarnilehto, H. Chapman, K. Kuokkanen, H. Wei, H. Viisanen, K.E. Akerman, K. Lindstedt, and A. Pertovaara. (2012) Inhibiting TRPA1 ion channel reduces loss of cutaneous nerve fiber function in diabetic animals: sustained activation of the TRPA1 channel contributes to the pathogenesis of peripheral diabetic neuropathy. Pharmacol Res. **65**(1), 149-58.
10. Kamiya, H., Y. Murakawa, W. Zhang, and A.A. Sima. (2005) Unmyelinated fiber sensory neuropathy differs in type 1 and type 2 diabetes. Diabetes Metab Res Rev. **21**(5), 448-58.
11. Pawson, E.J., B. Duran-Jimenez, R. Surosky, H.E. Brooke, S.K. Spratt, D.R. Tomlinson, and N.J. Gardiner. (2010) Engineered zinc finger protein-mediated VEGF-a activation restores deficient VEGF-a in sensory neurons in experimental diabetes. Diabetes. **59**(2), 509-18.
12. Verheyen, A., E. Peeraer, D. Lambrechts, K. Poesen, P. Carmeliet, M. Shibuya, I. Pintelon, J.P. Timmermans, R. Nuydens, and T. Meert. (2013) Therapeutic potential of VEGF and VEGF-derived peptide in peripheral neuropathies. Neuroscience. **244**, 77-89.
13. Beazley-Long, N., J. Hua, T. Jehle, R.P. Hulse, R. Dersch, C. Lehrling, H. Bevan, Y. Qiu, W.A. Lagreze, D. Wynick, A.J. Churchill, P. Kehoe, S.J. Harper, D.O. Bates, and L.F. Donaldson. (2013) VEGF-A165b Is an Endogenous Neuroprotective Splice Isoform of Vascular Endothelial Growth Factor A in Vivo and in Vitro. Am J Pathol. **183**(3), 918-29.
14. Sondell, M., G. Lundborg, and M. Kanje. (1999) Vascular endothelial growth factor has neurotrophic activity and stimulates axonal outgrowth, enhancing cell survival and Schwann cell proliferation in the peripheral nervous system. J Neurosci. **19**(14), 5731-40.
15. Lin, J., G. Li, X. Den, C. Xu, S. Liu, Y. Gao, H. Liu, J. Zhang, X. Li, and S. Liang. (2010) VEGF and its receptor-2 involved in neuropathic pain transmission mediated by P2X(2/3) receptor of primary sensory neurons. Brain Res Bull. **83**(5), 284-91.
16. Hulse, R.P., N. Beazley-Long, J. Hua, H. Kennedy, J. Prager, H. Bevan, Y. Qiu, E.S. Fernandes, M.V. Gammons, K. Ballmer-Hofer, A.C. Gittenberger de Groot, A.J. Churchill, S.J. Harper, S.D. Brain, D.O. Bates, and L.F. Donaldson. (2014) Regulation

of alternative VEGF-A mRNA splicing is a therapeutic target for analgesia. Neurobiol Dis. **71**, 245-59.

17. Kawamura, H., X. Li, K. Goishi, L.A. van Meeteren, L. Jakobsson, S. Cebe-Suarez, A. Shimizu, D. Edholm, K. Ballmer-Hofer, L. Kjellen, M. Klagsbrun, and L. Claesson-Welsh. (2008) Neuropilin-1 in regulation of VEGF-induced activation of p38MAPK and endothelial cell organization. Blood. **112**(9), 3638-49.
18. Woolard, J., W.Y. Wang, H.S. Bevan, Y. Qiu, L. Morbidelli, R.O. Pritchard-Jones, T.G. Cui, M. Sugiono, E. Waine, R. Perrin, R. Foster, J. Digby-Bell, J.D. Shields, C.E. Whittles, R.E. Mushens, D.A. Gillatt, M. Ziche, S.J. Harper, and D.O. Bates. (2004) VEGF165b, an inhibitory vascular endothelial growth factor splice variant: mechanism of action, in vivo effect on angiogenesis and endogenous protein expression. Cancer Res. **64**(21), 7822-35.
19. Quattrini, C., M. Jeziorska, A.J. Boulton, and R.A. Malik. (2008) Reduced vascular endothelial growth factor expression and intra-epidermal nerve fiber loss in human diabetic neuropathy. Diabetes Care. **31**(1), 140-5.
20. Calcutt, N.A., Modeling Diabetic Sensory Neuropathy in Rats, in Pain Research: Methods and Protocols, Z.D. Luo, Editor. 2004. p. 55-65.
21. Drake, R.A., R.P. Hulse, B.M. Lumb, and L.F. Donaldson. (2014) The degree of acute descending control of spinal nociception in an area of primary hyperalgesia is dependent on the peripheral domain of afferent input. J Physiol. **592**(16), 3611-24.
22. Hargreaves, K., R. Dubner, F. Brown, C. Flores, and J. Joris. (1988) A new and sensitive method for measuring thermal nociception in cutaneous hyperalgesia. Pain. **32**(1), 77-88.
23. Hamilton, R.T., A. Bhattacharya, M.E. Walsh, Y. Shi, R. Wei, Y. Zhang, K.A. Rodriguez, R. Buffenstein, A.R. Chaudhuri, and H. Van Remmen. (2013) Elevated protein carbonylation, and misfolding in sciatic nerve from db/db and Sod1(-/-) mice: plausible link between oxidative stress and demyelination. PLoS One. **8**(6), e65725.
24. Xu, Q., T. Qaum, and A.P. Adamis. (2001) Sensitive blood-retinal barrier breakdown quantitation using Evans blue. Invest Ophthalmol Vis Sci. **42**(3), 789-94.
25. Russell, J.W., D. Golovoy, A.M. Vincent, P. Mahendru, J.A. Olzmann, A. Mentzer, and E.L. Feldman. (2002) High glucose-induced oxidative stress and mitochondrial dysfunction in neurons. Faseb J. **16**(13), 1738-48.
26. Chen, W., R. Mi, N. Haughey, M. Oz, and A. Hoke. (2007) Immortalization and characterization of a nociceptive dorsal root ganglion sensory neuronal line. J Peripher Nerv Syst. **12**(2), 121-30.
27. Arimura, A., T. Deguchi, K. Sugimoto, T. Uto, T. Nakamura, Y. Arimura, K. Arimura, S. Yagihashi, Y. Nishio, and H. Takashima. (2013) Intraepidermal nerve fiber density and nerve conduction study parameters correlate with clinical staging of diabetic polyneuropathy. Diabetes Res Clin Pract. **99**(1), 24-9.
28. Casanova-Molla, J., M. Morales, E. Planas-Rigol, A. Bosch, M. Calvo, J.M. Grau-Junyent, and J. Valls-Sole. (2012) Epidermal Langerhans cells in small fiber neuropathies. Pain. **153**(5), 982-9.
29. Ohta, T., T. Imagawa, and S. Ito. (2007) Novel agonistic action of mustard oil on recombinant and endogenous porcine transient receptor potential V1 (pTRPV1) channels. Biochem Pharmacol. **73**(10), 1646-56.
30. Islam, M.S., D. Koya, and B. Portha. (2013) Animal models of diabetes and its associated complications. J Diabetes Res. **2013**, 593204.
31. Galloway, C. and M. Chattopadhyay. (2013) Increases in inflammatory mediators in DRG implicate in the pathogenesis of painful neuropathy in Type 2 diabetes. Cytokine. **63**(1), 1-5.
32. Ragavendran, J.V., A. Laferriere, W.H. Xiao, G.J. Bennett, S.S. Padi, J. Zhang, and T.J. Coderre. (2013) Topical combinations aimed at treating microvascular dysfunction reduce allodynia in rat models of CRPS-I and neuropathic pain. J Pain. **14**(1), 66-78.
33. Habib, A.A. and T.H. Brannagan, 3rd. (2010) Therapeutic strategies for diabetic neuropathy. Curr Neurol Neurosci Rep. **10**(2), 92-100.

34. Hamzeh, H., A. Gaudillere, O. Sabido, I. Tchou, C. Lambert, D. Schmitt, C. Genin, and L. Misery. (2000) Expression of PGP9.5 on Langerhans' cells and their precursors. Acta Derm Venereol. **80**(1), 14-6.
35. Simard, B., B.H. Gabra, and P. Sirois. (2002) Inhibitory effect of a novel bradykinin B1 receptor antagonist, R-954, on enhanced vascular permeability in type 1 diabetic mice. Can J Physiol Pharmacol. **80**(12), 1203-7.
36. Zochodne, D.W. (1996) Is early diabetic neuropathy a disorder of the dorsal root ganglion? A hypothesis and critique of some current ideas on the etiology of diabetic neuropathy. J Peripher Nerv Syst. **1**(2), 119-30.
37. Ibrahim, S., N.D. Harris, M. Radatz, F. Selmi, S. Rajbhandari, L. Brady, J. Jakubowski, and J.D. Ward. (1999) A new minimally invasive technique to show nerve ischaemia in diabetic neuropathy. Diabetologia. **42**(6), 737-42.
38. Perrin, R.M., O. Konopatskaya, Y. Qiu, S. Harper, D.O. Bates, and A.J. Churchill. (2005) Diabetic retinopathy is associated with a switch in splicing from anti- to pro-angiogenic isoforms of vascular endothelial growth factor. Diabetologia. **48**(11), 2422-7.
39. Tremolada, G., R. Lattanzio, G. Mazzolari, and G. Zerbini. (2007) The therapeutic potential of VEGF inhibition in diabetic microvascular complications. Am J Cardiovasc Drugs. **7**(6), 393-8.
40. Materazzi, S., C. Fusi, S. Benemei, P. Pedretti, R. Patacchini, B. Nilius, J. Prenen, C. Creminon, P. Geppetti, and R. Nassini. (2012) TRPA1 and TRPV4 mediate paclitaxel-induced peripheral neuropathy in mice via a glutathione-sensitive mechanism. Pflugers Arch. **463**(4), 561-9.
41. McNamara, C.R., J. Mandel-Brehm, D.M. Bautista, J. Siemens, K.L. Deranian, M. Zhao, N.J. Hayward, J.A. Chong, D. Julius, M.M. Moran, and C.M. Fanger. (2007) TRPA1 mediates formalin-induced pain. Proc Natl Acad Sci U S A. **104**(33), 13525-30.
42. Ferrari, L.F., O. Bogen, and J.D. Levine. (2010) Nociceptor subpopulations involved in hyperalgesic priming. Neuroscience. **165**(3), 896-901.
43. Meseguer, V., Y.A. Alpizar, E. Luis, S. Tajada, B. Denlinger, O. Fajardo, J.A. Manenschijn, C. Fernandez-Pena, A. Talavera, T. Kichko, B. Navia, A. Sanchez, R. Senaris, P. Reeh, M.T. Perez-Garcia, J.R. Lopez-Lopez, T. Voets, C. Belmonte, K. Talavera, and F. Viana. (2014) TRPA1 channels mediate acute neurogenic inflammation and pain produced by bacterial endotoxins. Nat Commun. **5**, 3125.
44. Bates, D.O., N.J. Hillman, B. Williams, C.R. Neal, and T.M. Pocock. (2002) Regulation of microvascular permeability by vascular endothelial growth factors. J Anat. **200**(6), 581-97.
45. Tsantoulas, C., L. Zhu, Y. Shaifta, J. Grist, J.P. Ward, R. Raouf, G.J. Michael, and S.B. McMahon. (2012) Sensory neuron downregulation of the Kv9.1 potassium channel subunit mediates neuropathic pain following nerve injury. J Neurosci. **32**(48), 17502-13.
46. Dunham, J.P., S. Kelly, and L.F. Donaldson. (2008) Inflammation reduces mechanical thresholds in a population of transient receptor potential channel A1-expressing nociceptors in the rat. Eur J Neurosci. **27**(12), 3151-60.
47. Barriere, D.A., J. Rieusset, D. Chanteranne, J. Busserolles, M.A. Chauvin, L. Chapuis, J. Salles, C. Dubray, and B. Morio. (2012) Paclitaxel therapy potentiates cold hyperalgesia in streptozotocin-induced diabetic rats through enhanced mitochondrial reactive oxygen species production and TRPA1 sensitization. Pain. **153**(3), 553-61.
48. Eberhardt, M.J., M.R. Filipovic, A. Leffler, J. de la Roche, K. Kistner, M.J. Fischer, T. Fleming, K. Zimmermann, I. Ivanovic-Burmazovic, P.P. Nawroth, A. Bierhaus, P.W. Reeh, and S.K. Sauer. (2012) Methylglyoxal activates nociceptors through transient receptor potential channel A1 (TRPA1): a possible mechanism of metabolic neuropathies. J Biol Chem. **287**(34), 28291-306.
49. Nowak, D.G., J. Woolard, E.M. Amin, O. Konopatskaya, M.A. Saleem, A.J. Churchill, M.R. Ladomery, S.J. Harper, and D.O. Bates. (2008) Expression of pro- and anti-

angiogenic isoforms of VEGF is differentially regulated by splicing and growth factors. J Cell Sci. **121**(Pt 20), 3487-95.

Figure legends

Figure 1. VEGF-A_{165}b reverses diabetic neuropathic pain behaviours in rats.

A. Blood glucose levels measured in the STZ-treated animals (STZ injection on day 0, open circles) compared to age matched naïve (vehicle injected, closed circles) animals. B. The body weights of the groups. Two experimental groups of diabetic (STZ) animals were treated with either vehicle or VEGF-A_{165}b during week 1 (arrowhead) and treatment was continued biweekly until duration of the experiment. STZ treatment led to neuropathic pain phenotypes in the diabetic + vehicle group, demonstrated by C. Mechanical allodynia measured by von Frey hair withdrawal threshold. D. cold allodynia measured by withdrawal to acetone. E. heat hyperalgesia measured by latency of withdrawal. F. Acute response to 0.5% formalin (0-15 min) in diabetic rats after two weeks. VEGF-A_{165}b treatment attenuated diabetic neuropathic pain (C-F). (2 way ANOVA + Bonferroni multiple comparisons test *p<0.05, **p<0.01, ***p<0.001 compared to diabetic group, naïve n=6, diabetic n=9, diabetic + VEGF-A_{165}b n=7). Note that the same symbols are used in all graphs for the different groups of animals.

Figure 2. A. Primary adult DRG neurons stained for NSE-1 (green) and AC3 (red) in different experimental conditions. B. The percentage of AC3 expressing cells was increased by high glucose treatment and blocked by VEGF-A_{165}b treatment (n=4, scale bars = 25µm). C. Images of L5 DRG expressing AC3 from naïve, diabetic (D & E, scale bar = 50µm), diabetic + VEGF-A_{165}b & negative controls. D. AC3 expression significantly increased in diabetic animals (n=3) but not in VEGF-A_{165}b treated diabetic animals. E. AC3 expression by neuronal size. AC3 expression was increased in small/medium L5 DRG neuronal cell bodies (<400µm^2, 401-800 µm^2) in diabetic animals (n=3), and was partially ameliorated by VEGF-A_{165}b. F. The percentage of total neuronal cell bodies by size with an area less than 400µm^2 was increased in diabetic animals compared to naïve. VEGF-A_{165}b treatment prevented this effect of diabetes on DRG neuronal cell body cross-sectional area. (2 way ANOVA + Bonferroni multiple comparisons *p<0.05, **p<0.01, ***p<0.001.)

Figure 3. A. AC3 expression in isolectin-B4 (IB4) positive neurons. B. The number of IB4 positive neurons expressing AC3 was increased in diabetic and reduced in VEGF-A_{165}b treated rats. C. AC3 expression in neurofilament (NF200)+ve DRG subsets. D. This was increased in diabetic compared to naïve was reduced in diabetics + VEGF-A_{165}b (n=3/group, Kruskal Wallis test *p<0.05.)

Figure 4. A. Representative images of epidermal/dermal (dashed line) nerve innervation (arrows) and Langerhans cells (arrowheads) stained with PGP9.5 in plantar skin from naïve, diabetic and VEGF-A_{165}b treated diabetic rats. Nerves and Langerhans cells were quantified in the same sections. B. There was a lower dermal/epidermal border innervation density in diabetic animals that was reversed by VEGF-A_{165}b treatment. C. Diabetic animals had increased intra-epidermal Langerhans cell numbers, which was prevented by VEGF-A_{165}b treatment. (n=3, Kruskal Wallis test *p<0.05, **p<0.01, ***p<0.001. Scale bar = 50µm.)

Figure 5. A-C. Sciatic nerves from naïve, diabetic and VEGF-A_{165}b treated animals were stained with toluidine blue. B. Myelinated fibre cross-sectional area was reduced in diabetes, which was prevented by long-term systemic administration of VEGF-A_{165}b (n=3/group, scale bar = 50µm). C. Myelinated nerve fibre numbers broken down by cross sectional area. D

Higher power image of axons demonstrating aberrant myelin morphology (* in A). E. The percentage of aberrant axons was increased in diabetic animals and inhibited by VEGF-A_{165}b treatment. Scale bars = 20µm, 10µm. F. NF200 staining of DRG neurons in normal, diabetic and VEGF-A_{165}b treated animals. G. The cross-sectional area profile of NF200+ve DRG neuronal cell bodies was significantly different in L5 DRG of diabetic animals compared to naïve, a difference that was not observed with VEGF-A_{165}b treatment. (Kruskal Wallis test and two way ANOVA with Bonferroni multiple comparisons test were performed. **p<0.01, ***p<0.001.)

Figure 6. Evans blue extravasation was increased in diabetic nerves and reduced by VEGF-A_{165}b. A. Animals were perfused with Evans blue for 2 hours and the extravasation (tissue dye as a proportion of plasma dye concentration, per hour per gram of tissue) quantified by spectroscopy. STZ increased Evans Blue extravasation (displayed as permeability-surface area coefficient (PA)) (n=5) that increased in diabetes and reduced by long-term systemic VEGF-A_{165}b treatment in A. L3, L4 & L5 DRG, B. saphenous nerve and C. plantar skin (n=5, Kruskal Wallis test *p<0.05 **p<0.01).

Figure 7. Cultured, differentiated 50B11 immortalised DRG neurons were loaded with the calcium indicator dye Fluo4, treated with the TRPA1 agonist AITC and fluorescence intensity measured and normalized to baseline. A. AITC evoked a concentration-dependent increase in intracellular calcium, (n=5). Cells were pre-treated with the TRPA1 antagonist AP-18 (100µM). B. 50B11s express VEGFR2, which is unaltered by glucose concentration. C & D. The response to 100 µM AITC was blocked by AP-18. E & F. Cells were pre-treated with VEGF-A_{165}b overnight and the calcium response to 100µM AITC measured. The TRPA1 calcium increase was significantly reduced by overnight pre-treatment with VEGF-A_{165}b (n=8). G. 50B11 cells were treated for 24h with 300µM AITC and stained for AC3. H. AC3 fluorescence intensity was increased by AITC. (A,C-F, 2 way ANOVA + Bonferroni multiple comparisons test, Kruskal Wallis test and F. Mann Whitney test *p<0.05, **p<0.01, ***p<0.001, ****p<0.0001).

Figure 8. A. Cultured, differentiated 50B11 immortalised DRG neurons were treated with high glucose treatment for 24h and AC3 expression determined by immunofluorescence. B. High glucose increased AC3 expression. C. Cells were treated with AITC after incubation in basal glucose medium or high glucose, and calcium measured by Fluo4 fluorescence intensity. D. High glucose enhanced the sustained increase in intracellular calcium in the presence of AITC, compared to basal glucose, which was not attributable to an osmotic effect, as mannitol had no effect (n=10). E. Cells were pre-treated with high glucose, with or without VEGF-A_{165}b, or inhibitors and calcium measured in response to AITC. F. VEGF-A_{165}b blocked the increase in calcium induced by AITC in high glucose conditions (n=9), and this was inhibited by G. the VEGF receptor antagonist PTK787, 200nM (n=13) and H. the specific VEGFR2 neutralizing antibody DC101, 8.05µg/mL (n=7). All experimental culture conditions are displayed on the x axes. (2 way ANOVA + Bonferroni multiple comparisons test, Kruskal Wallis test and Mann Whitney tests *p<0.05, **p<0.01, ***p<0.001, ****p<0.0001).

Running title: VEGF-A_{165}b prevents diabetic neuropathic pain

Summary statement (<40 words)
Systemic treatment of diabetic rats with a novel human growth factor, VEGF-A_{165}b, reversed neuropathic pain and peripheral nerve damage.

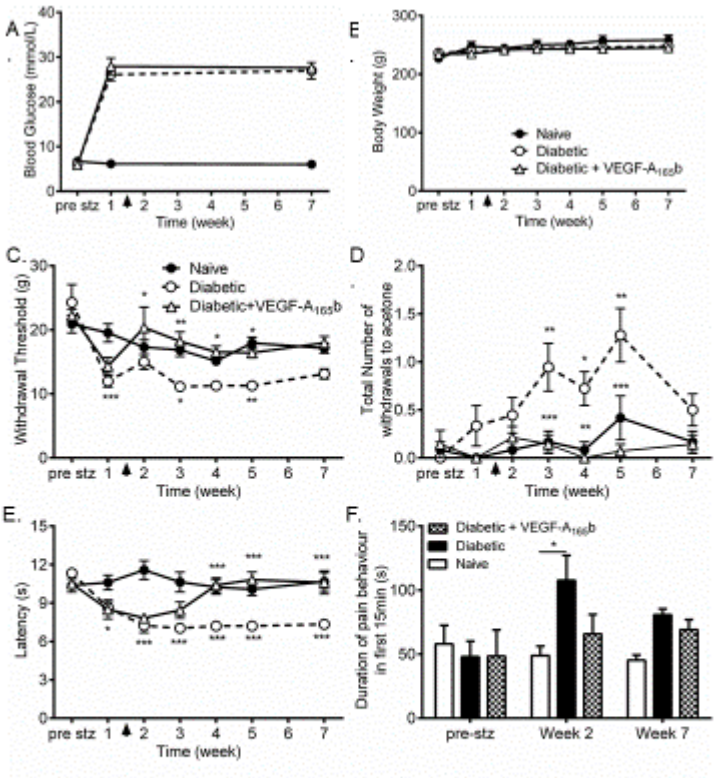
A.
Blood Glucose (mmol/L)
pre stz 1 2 3 4 5 6 7
Time (week)
B.
Body Weight (g)
Naive
Diabetic
Diabetic + VEGF-A165b
pre stz 1 2 3 4 5 6 7
Time (week)
C.
Withdrawal Threshold (g)
Naive
Diabetic
Diabetic+VEGF-A165b
pre stz 1 2 3 4 5 6 7
Time (week)
D.
Total Number of withdrawals to acetone
pre stz 1 2 3 4 5 6 7
Time (week)
E.
Latency (s)
pre stz 1 2 3 4 5 6 7
Time (week)
F.
Duration of pain behaviour in first 15min (s)
Diabetic + VEGF-A165b
Diabetic
Naive
pre-stz
Week 2
Week 7

Figure 1

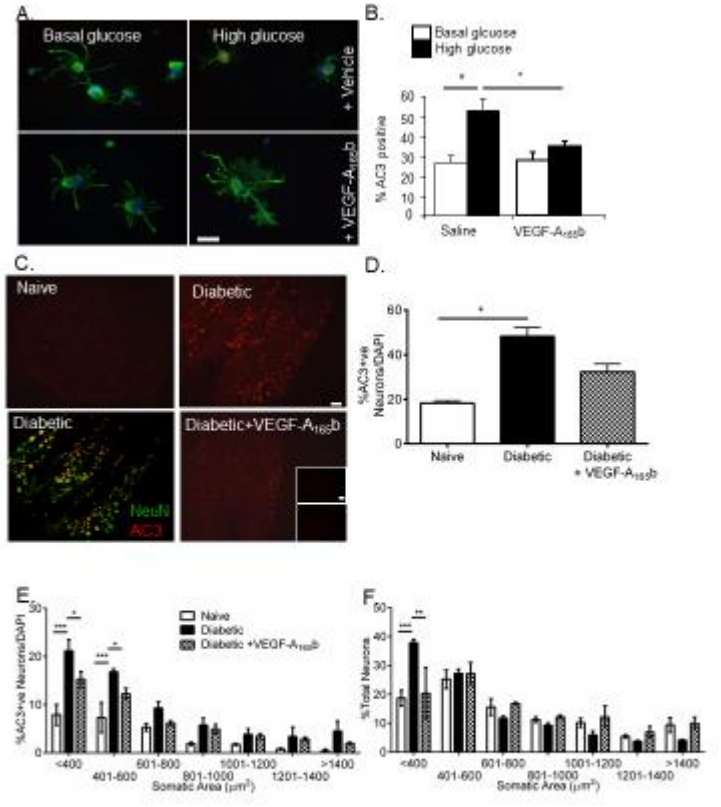
A.
Basal glucose
High glucose
+ Vehicle
+ VEGF-A165b
B.
Basal glucose
High glucose
% AC3 positive
Saline
VEGF-A165b
C.
Naive
Diabetic
Diabetic
Diabetic+VEGF-A165b
NeuN
AC3
D.
%AC3+ve Neurons/DAPI
Naive
Diabetic
Diabetic + VEGF-A165b
E
%AC3+ve Neurons/DAPI
Naive
Diabetic
Diabetic +VEGF-A165b
<400
401-600
601-800
801-1000
1001-1200
1201-1400
>1400
Somatic Area (μm²)
F
% Total Neurons
<400
401-600
601-800
801-1000
1001-1200
1201-1400
>1400
Somatic Area (μm²)

Figure 2

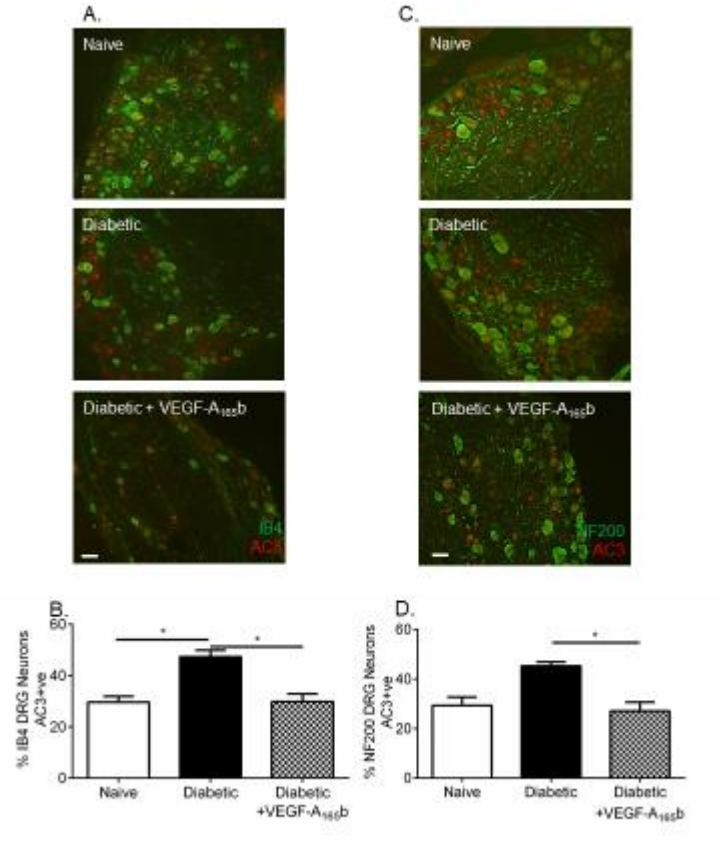
A.
Naive
Diabetic
Diabetic + VEGF-A165b
IB4
AC3
C.
Naive
Diabetic
Diabetic + VEGF-A165b
NF200
AC3
B.
% IB4 DRG Neurons AC3+ve
60
40
20
0
Naive
Diabetic
Diabetic +VEGF-A165b
D.
% NF200 DRG Neurons AC3+ve
60
40
20
0
Naive
Diabetic
Diabetic +VEGF-A165b

Figure 3

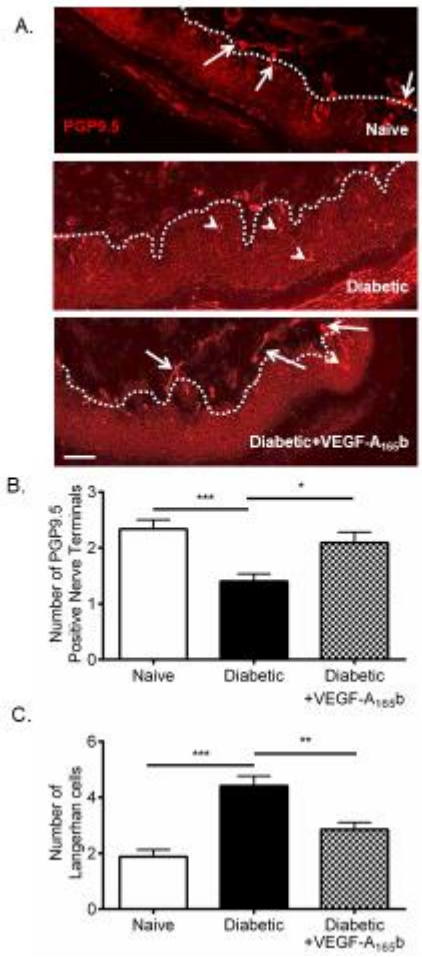
A.
PGP9.5
Naive
Diabetic
Diabetic+VEGF-A165b
B.
Number of PGP9.5 Positive Nerve Terminals
***
*
Naive
Diabetic
Diabetic +VEGF-A165b
C.
Number of Langerhan cells
***
**
Naive
Diabetic
Diabetic +VEGF-A165b

Figure 4

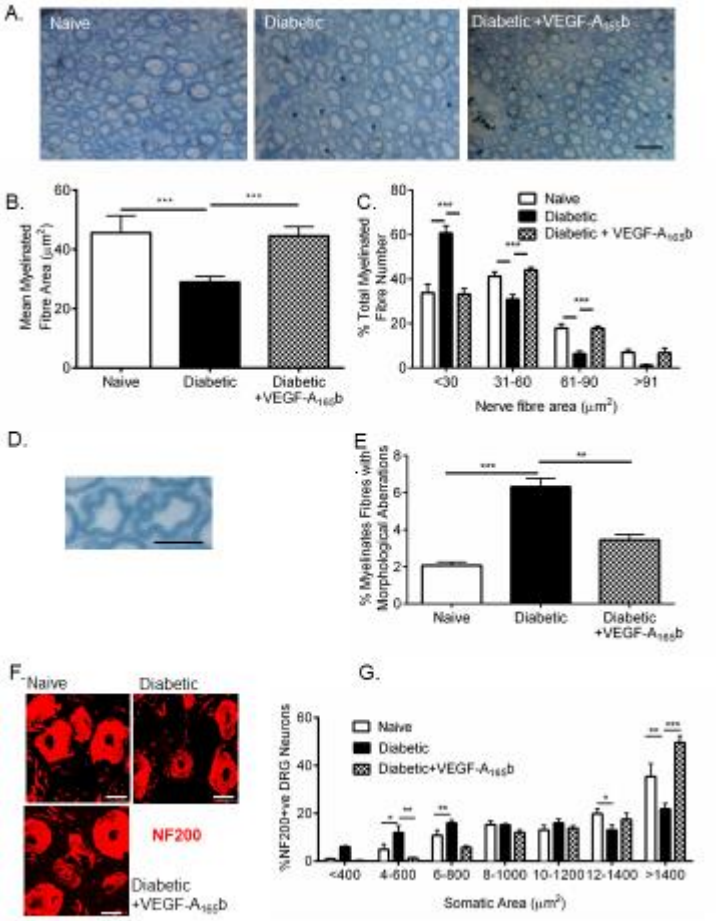
A.
Naive
Diabetic
Diabetic +VEGF-A165b
B.
Mean Myelinated Fibre Area (μm²)
Naive
Diabetic
Diabetic +VEGF-A165b
C.
% Total Myelinated Fibre Number
Naive
Diabetic
Diabetic + VEGF-A165b
<30
31-60
61-90
>91
Nerve fibre area (μm²)
D.
E.
% Myelinates Fibres with Morphological Aberrations
Naive
Diabetic
Diabetic +VEGF-A165b
F.
Naive
Diabetic
NF200
Diabetic +VEGF-A165b
G.
%NF200+ve DRG Neurons
Naive
Diabetic
Diabetic+VEGF-A165b
<400
4-600
6-800
8-1000
10-1200
12-1400
>1400
Somatic Area (μm²)

Figure 5

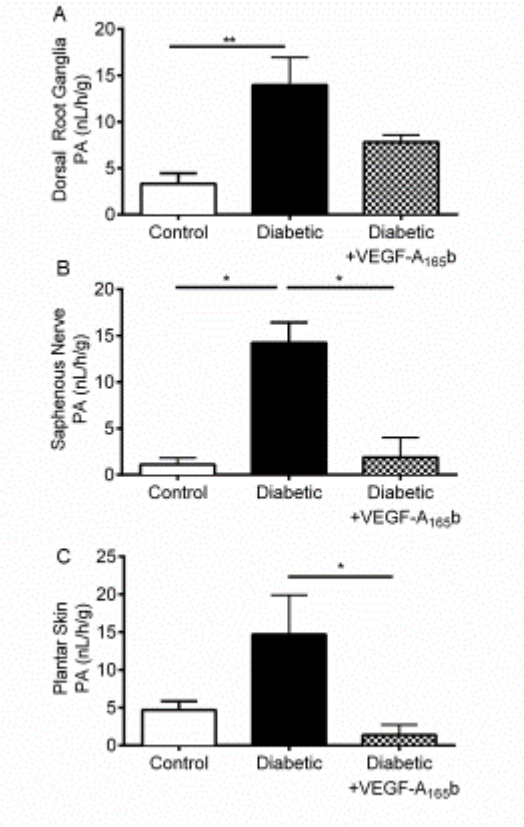
A
Dorsal Root Ganglia PA (nL/h/g)
20
15
10
5
0
**
Control
Diabetic
Diabetic +VEGF-A165b
B
Saphenous Nerve PA (nL/h/g)
20
15
10
5
0
*
*
Control
Diabetic
Diabetic +VEGF-A165b
C
Plantar Skin PA (nL/h/g)
25
20
15
10
5
0
*
Control
Diabetic
Diabetic +VEGF-A165b

Figure 6

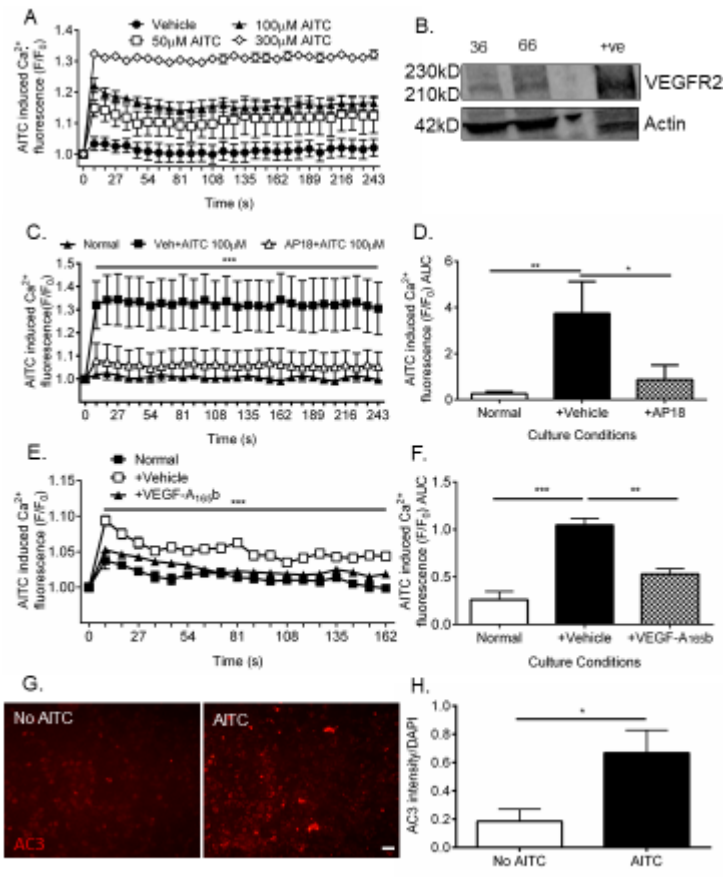
A
Vehicle
100μM AITC
50μM AITC
300μM AITC
AITC induced Ca2+ fluorescence (F/F0)
Time (s)
B.
36
66
+ve
230kD
210kD
42kD
VEGFR2
Actin
C.
Normal
Veh+AITC 100μM
AP18+AITC 100μM
D.
AITC induced Ca2+ fluorescence (F/F0) AUC
Normal
+Vehicle
+AP18
Culture Conditions
E.
Normal
+Vehicle
+VEGF-A165b
F.
+VEGF-A165b
G.
No AITC
AITC
AC3
H.
AC3 intensity/DAPI

Figure 7

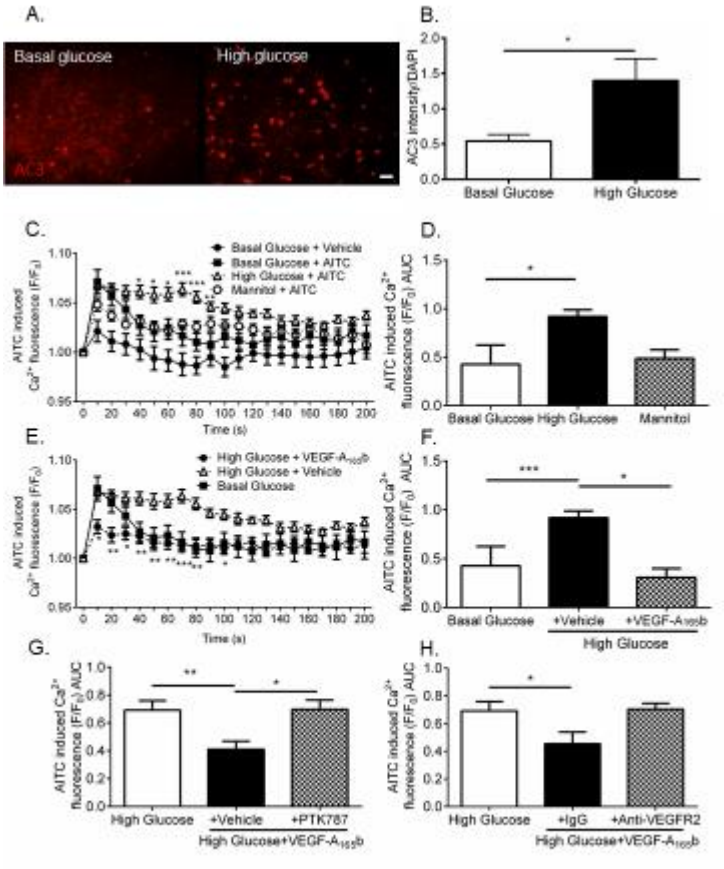
A.
Basal glucose
High glucose
AC3
B.
AC3 intensity/DAPI
Basal Glucose
High Glucose
C.
Basal Glucose + Vehicle
Basal Glucose + AITC
High Glucose + AITC
Mannitol + AITC
AITC induced Ca2+ fluorescence (F/F0)
Time (s)
D.
AITC induced Ca2+ fluorescence (F/F0) AUC
Basal Glucose
High Glucose
Mannitol
E.
High Glucose + VEGF-A165b
High Glucose + Vehicle
Basal Glucose
F.
Basal Glucose
+Vehicle
+VEGF-A165b
High Glucose
G.
High Glucose
+Vehicle
+PTK787
High Glucose+VEGF-A165b
H.
High Glucose
+IgG
+Anti-VEGFR2
High Glucose+VEGF-A165b

Figure 8